

Generalized second law of thermodynamics on the apparent horizon in modified Gauss-Bonnet gravity

A. Abdolmaleki^{1*}, T. Najafi^{2†},

¹Center for Excellence in Astronomy & Astrophysics of Iran (CEAAI-RIAAM), Maragha, Iran

²Department of Physics, University of Kurdistan, Pasdaran St., Sanandaj, Iran

October 7, 2018

Abstract

Modified gravity and generalized second law (GSL) of thermodynamics are interesting topics in the modern cosmology. In this regard, we investigate the GSL of gravitational thermodynamics in the framework of modified Gauss-Bonnet gravity or $f(G)$ -gravity. We consider a spatially FRW universe filled with the matter and radiation enclosed by the dynamical apparent horizon with the Hawking temperature. For two viable $f(G)$ models, we first numerically solve the set of differential equations governing the dynamics of $f(G)$ -gravity. Then, we obtain the evolutions of the Hubble parameter, the Gauss-Bonnet curvature invariant term, the density and equation of state parameters as well as the deceleration parameter. In addition, we check the energy conditions for both models and finally examine the validity of the GSL. For the selected $f(G)$ models, we conclude that both models have a stable de Sitter attractor. The equation of state parameters behave quite similar to those of the Λ CDM model in the radiation/matter dominated epochs, then they enter the phantom region before reaching the de Sitter attractor with $\omega = -1$. The deceleration parameter starts from the radiation/matter dominated eras, then transits from a cosmic deceleration to acceleration and finally approaches a de Sitter regime at late times, as expected. Furthermore, the GSL is respected for both models during the standard radiation/matter dominated epochs. Thereafter when the universe becomes accelerating, the GSL is violated in some ranges of scale factor. At late times, the evolution of the GSL predicts an adiabatic behavior for the accelerated expansion of the universe.

PACS numbers: 04.50.Kd

Keywords: modified gravity

*AAbdolmaleki@uok.ac.ir

†t.najafi90@gmail.com

1 Introduction

Various cosmological observations, coming from the type Ia supernovae (SNeIa) surveys [1], the large scale structure (LSS) [2], the cosmic microwave background (CMB) anisotropy spectrum [3, 4] and the Hubble parameter $H(z)$ [5], have indicated that the universe is in a phase of accelerated expansion. Regarding the accelerated expansion of the universe, there are two main categories of probable solutions. One is to assume that in the context of general relativity (GR), the universe is dominated by a new cosmic fluid with negative pressure. This kind of exotic matter which violates the strong energy condition is so called “dark energy“ (DE) [6, 7]. Another alternative, originates from the modification of gravity [8]. In modified gravity (MG) theories, there is no require for DE with exclusive properties, but instead, the action contains a general function of invariants obtained from the Riemann curvature tensor such as the Ricci scalar, R , [9] or the Gauss-Bonnet invariant term, G , [10] or the torsion scalar, T [11]. Moreover, in [12] it was shown that MG may serve as dark matter (DM).

One of interesting alternative theories of gravity is modified Gauss-Bonnet gravity, so-called $f(G)$ -gravity, where $f(G)$ is a general function of the Gauss-Bonnet curvature invariant term $G = R^2 - 4R_{\mu\nu}R^{\mu\nu} + R_{\mu\nu\rho\sigma}R^{\mu\nu\rho\sigma}$ [10, 13, 14, 15, 16, 17, 18]. The $f(G)$ -gravity can justify the present accelerated expansion of the universe without resorting to DE. Besides, it can also describe the phantom divide line crossing as well as the cosmic transition from deceleration to acceleration phase [19, 20, 21]. The cosmologically viable $f(G)$ models need to be close to the Λ CDM model in the deep matter era, but the deviation from it becomes important at late times on cosmological scales. An appreciable deviation from the Λ CDM cosmology yields the modification of the matter power spectrum, which can be used as a crucial tool to distinguish $f(G)$ -gravity from the Λ CDM model.

Additionally, the thermodynamical interpretation of gravity is one of another interesting topics in modern cosmology. From the viewpoint of the physics of the black holes, there is a deep rooted connection between thermodynamics and gravity [22]. This connection was first discovered in the Einstein gravity for the Rindler spacetime [23]. It was also shown that by assuming the geometric entropy given by a quarter of the apparent horizon area of a Friedmann-Robertson-Walker (FRW) universe, the Friedmann equation in the Einstein gravity can be written in the form of the first law of thermodynamics [24]. The connection between thermodynamics and gravity has also been investigated in $f(R)$ -gravity and scalar-tensor theory [25], $f(T)$ -gravity [26], Lovelock theory [27] and braneworld scenarios (such as DGP, RSI and RSII) [28].

It is also of great interest to generalize our discussion to study the generalized second law (GSL) of thermodynamics. The GSL states that the entropy of matter inside the horizon of the universe plus the geometric entropy of the horizon is non-decreasing with time [24]. Note that the ordinary second law of thermodynamics only deals with the entropy of matter inside the universe. In the Einstein gravity, it was shown that the GSL in the presence of DE is always satisfied [29]. The validity of the GSL was also examined in different theories of MG [29]-[37]. Here our main aim is to explore the GSL and the thermodynamics of the apparent horizon in $f(G)$ -gravity, and obtain the condition for the GSL to be satisfied. The paper is structured as follows. In section 2, we briefly review the $f(G)$ -gravity. In section 3, we investigate the GSL of thermodynamics on the dynamical apparent horizon with the Hawking temperature. In section 4, we study the dynamics of $f(G)$ -gravity. In section 5, we give numerical results obtained for the evolution of some cosmological parameters, check the energy conditions and examine the validity of the GSL for two viable $f(G)$ models. Section 6 is devoted to conclusions.

2 THE $f(G)$ THEORY OF GRAVITY

The action of modified Gauss-Bonnet gravity is given by [14]:

$$I = \int d^4x \sqrt{-g} \left(\frac{1}{2k^2} R + f(G) + L_r + L_m \right), \quad (1)$$

where $k^2 = 8\pi G_N = 1$ and G_N is the Newtonian gravitational constant. Also g , R , L_r , L_m and $f(G)$ are the determinant of metric $g_{\mu\nu}$, Ricci scalar, the matter Lagrangian, the radiation Lagrangian and a general function of the Gauss-Bonnet term, respectively. The Gauss-Bonnet curvature invariant term is defined as

$$G = R^2 - 4R_{\mu\nu}R^{\mu\nu} + R_{\mu\nu\rho\sigma}R^{\mu\nu\rho\sigma}. \quad (2)$$

Taking variation of the action (1) with respect to $g_{\mu\nu}$ leads to the field equations

$$\begin{aligned} T_{\mu\nu} = R_{\mu\nu} - \frac{1}{2}Rg_{\mu\nu} + 8[R_{\mu\rho\nu\sigma} + R_{\rho\nu}g_{\sigma\mu} - R_{\rho\sigma}g_{\nu\mu} - R_{\mu\nu}g_{\sigma\rho} + R_{\mu\sigma}g_{\nu\rho} \\ + \frac{1}{2}R(g_{\mu\nu}g_{\sigma\rho} - g_{\mu\sigma}g_{\nu\rho})]\nabla^\rho\nabla^\sigma f_G + (Gf_G - f)g_{\mu\nu}, \end{aligned} \quad (3)$$

where $f_G = df/dG$. Also $T_{\mu\nu}$ and ∇^ρ are the energy-momentum tensor and the covariant derivative operator, respectively. Now we consider a spatially flat universe described by the FRW metric

$$ds^2 = -dt^2 + a^2(t)(dx^2 + dy^2 + dz^2), \quad (4)$$

where $a(t)$ is the scale factor. Consequently, we have

$$R = 6(\dot{H} + 2H^2), \quad G = 24H^2(\dot{H} + H^2), \quad (5)$$

where $H = \dot{a}/a$ is the Hubble parameter and an overdot stands for a derivative with respect to the cosmic time t . In terms of the deceleration parameter $q = -1 - \dot{H}/H^2$, Eq. (5) can be written as

$$R = 6H^2(1 - q), \quad G = 24H^4q. \quad (6)$$

Substituting the FRW metric (4) into the field equations (3) yields the Friedmann equations in $f(G)$ -gravity as

$$3H^2 = Gf_G - f - 24H^3\dot{f}_G + \rho_r + \rho_m, \quad (7)$$

$$-2\dot{H} = -8H^3\dot{f}_G + 16H\dot{H}\dot{f}_G + 8H^2\ddot{f}_G + \frac{4}{3}\rho_r + \rho_m, \quad (8)$$

where ρ_m and ρ_r are the energy density of matter and radiation, respectively.

The Friedmann equations (7) and (8) can be rewritten in the standard form as [38]

$$H^2 = \frac{1}{3}\rho_t, \quad (9)$$

$$\dot{H} = -\frac{1}{2}(\rho_t + p_t), \quad (10)$$

where ρ_t and p_t are the total energy density and pressure defined as

$$\rho_t = \rho_m + \rho_r + \rho_G, \quad (11)$$

$$p_t = p_m + p_r + p_G. \quad (12)$$

Here ρ_G and p_G are the energy density and pressure due to the $f(G)$ contribution defined as

$$\rho_G = Gf_G - f - 24H^3\dot{f}_G, \quad (13)$$

$$p_G = 16H^3\dot{f}_G + 16H\dot{H}\dot{f}_G + 8H^2\ddot{f}_G - Gf_G + f. \quad (14)$$

By using of Eqs. (13) and (14), one can obtain the equation of state (EoS) parameter due to the $f(G)$ contribution as [14]

$$\omega_G = \frac{p_G}{\rho_G} = \frac{16H^3\dot{f}_G + 16H\dot{H}\dot{f}_G + 8H^2\ddot{f}_G - Gf_G + f}{Gf_G - f - 24H^3\dot{f}_G}. \quad (15)$$

Also from Eqs. (9) and (10), the effective EoS parameter can be obtained as

$$\omega_{\text{eff}} = -1 - \frac{2\dot{H}}{3H^2}. \quad (16)$$

Moreover, the continuity equations governing the pressureless matter ($p_m = 0$), the radiation ($p_r = \rho_r/3$) and the $f(G)$ contribution satisfy

$$\dot{\rho}_m + 3H\rho_m = 0, \quad (17)$$

$$\dot{\rho}_r + 4H\rho_r = 0, \quad (18)$$

$$\dot{\rho}_G + 3H(\rho_G + p_G) = 0. \quad (19)$$

Equations (7), (8), (17) and (18) determine the dynamics of the $f(G)$ -gravity system (1) in a homogeneous and isotropic background. We will study this issue in section 4.

3 GSL IN $f(G)$ -GRAVITY

Here, we are interested in exploring the GSL of gravitational thermodynamics in the context of $f(G)$ -gravity. To this aim, we consider a spatially flat FRW universe filled with the matter and radiation. We further assume that the boundary of the universe to be enclosed by the dynamical apparent horizon with the Hawking temperature. For a spatially flat FRW universe, the dynamical apparent horizon takes the form [39, 40]

$$\tilde{r}_A = H^{-1}, \quad (20)$$

which is same as the Hubble horizon. Following [24], the Hawking temperature on \tilde{r}_A is given by

$$T_A = \frac{1}{2\pi\tilde{r}_A} \left(1 - \frac{\dot{\tilde{r}}_A}{2H\tilde{r}_A} \right). \quad (21)$$

Now we are going to use the first law of thermodynamics to find the general condition needed to hold the GSL in $f(G)$ -gravity. The entropy of matter and radiation inside the horizon are given by the Gibbs equation [29]

$$T_A dS_m = dE_m + p_m dV, \quad (22)$$

$$T_A dS_r = dE_r + p_r dV, \quad (23)$$

where $E_m = \rho_m V$ and $E_r = \rho_r V$. Also $V = 4\pi\tilde{r}_A^3/3$ is the volume of the dynamical apparent horizon \tilde{r}_A containing the pressureless matter ($p_m = 0$) and radiation ($p_r = \rho_r/3$).

Taking time derivative of Eqs. (22) and (23) and using (17) and (18) one can get

$$T_A \dot{S} = 4\pi\tilde{r}_A^2 \left(\rho_m + \frac{4}{3}\rho_r \right) (\dot{\tilde{r}}_A - H\tilde{r}_A), \quad (24)$$

where $S = S_r + S_m$. Replacing ρ_m and ρ_r from Eqs. (7) and (8) into the above relation and using $\tilde{r}_A = H^{-1}$, one can obtain

$$T_A \dot{S} = \frac{2\pi(\dot{H} + H^2)}{H^4} [4\dot{H} - 16H(H^2 - 2\dot{H})\dot{f}_G + 16H^2\ddot{f}_G]. \quad (25)$$

The horizon entropy in $f(R, G)$ -gravity is given by [19]

$$S_A = -\pi \int \left(F_R \frac{\partial R}{\partial R_{\alpha\beta\gamma\rho}} + F_G \frac{\partial G}{\partial R_{\alpha\beta\gamma\rho}} \right) \varepsilon_{\alpha\beta}\varepsilon_{\gamma\rho} dA, \quad (26)$$

where $F_R = \frac{\partial F(R, G)}{\partial R}$, $F_G = \frac{\partial F(R, G)}{\partial G}$ and $A = 4\pi\tilde{r}_A^2$ is the area of the apparent horizon ($\tilde{r}_A = H^{-1}$). Also the quantity $\varepsilon_{\alpha\beta}$ is normalized as $\varepsilon^{\alpha\beta}\varepsilon_{\alpha\beta} = -2$ and antisymmetric under the exchange $\alpha \longleftrightarrow \beta$. It is the binormal vector to the bifurcation surface [19]. For the action (1) we have

$$F(R, G) = R + 2f(G), \quad (27)$$

therefore Eq. (26) yields

$$S_A = 8\pi^2 (H^{-2} + 8f_G). \quad (28)$$

Taking time derivative of Eq. (28) and using the Hawking temperature (21), one can derive the evolution of the horizon entropy as

$$T_A \dot{S}_A = \frac{2\pi(\dot{H} + 2H^2)}{H^4} (-2\dot{H} + 8H^3\dot{f}_G). \quad (29)$$

Summing up Eqs. (25) and (29), the GSL in $f(G)$ -gravity yields

$$T_A \dot{S}_{\text{tot}} = \frac{2\pi}{H^4} [2\dot{H}^2 + 8H\dot{H}(4\dot{H} + 3H^2)\dot{f}_G + 16H^2(\dot{H} + H^2)\ddot{f}_G], \quad (30)$$

where $S_{\text{tot}} = S_r + S_m + S_A$. Equation (30) shows that in $f(G)$ gravity, the validity of the GSL, i.e. $T_A \dot{S}_{\text{tot}} \geq 0$, depends on the explicit form of the $f(G)$ model. For the Einstein gravity ($f(G) = 0$), one can immediately find that the GSL (30) reduces to

$$T_A \dot{S}_{\text{tot}} = \frac{4\pi\dot{H}^2}{H^4} \geq 0, \quad (31)$$

which shows that the GSL is always fulfilled throughout history of the universe. In section 5, we examine the validity of the GSL (30) for two viable $f(G)$ -gravity models.

4 Dynamics of $f(G)$ -gravity

To study the dynamics of a general $f(G)$ model, we use the following dimensionless variables [14, 41]

$$x_1 = \frac{Gf_G}{3H^2}, \quad (32)$$

$$x_2 = -\frac{f}{3H^2}, \quad (33)$$

$$x_3 = -8H\dot{f}_G, \quad (34)$$

$$x_4 = \Omega_r = \frac{\rho_r}{3H^2}, \quad (35)$$

$$x_5 = \frac{G}{24H^4} = \frac{\dot{H}}{H^2} + 1, \quad (36)$$

$$x_6 = H. \quad (37)$$

With the help of above definitions and using Eqs. (7), (8), (17) and (18) one can get a set of first order differential equations governing a general $f(G)$ model as [14]

$$\frac{dx_1}{dN} = -x_3x_5 \left(1 + \frac{1}{m}\right) + 2x_1(1 - x_5), \quad (38)$$

$$\frac{dx_2}{dN} = \frac{x_3x_5}{m} + 2x_2(1 - x_5), \quad (39)$$

$$\frac{dx_3}{dN} = -x_3(1 + x_5) + 2x_5 + 1 - 3(x_1 + x_2) + x_4, \quad (40)$$

$$\frac{dx_4}{dN} = -2x_4(1 + x_5), \quad (41)$$

$$\frac{dx_5}{dN} = x_5 \left[4(1 - x_5) - \frac{x_3x_5}{mx_1}\right], \quad (42)$$

$$\frac{dx_6}{dN} = (x_5 - 1)x_6, \quad (43)$$

where $N = \ln(a/a_i)$ and a_i is the initial value of the scalar factor. Also

$$m = \frac{Gf_{GG}}{f_G}. \quad (44)$$

Notice that the variable $x_6 = H$, Eq. (37), and the differential equation (43) are absent in [14].

Using Eqs. (32)-(35), one can rewrite Eqs. (7) and (13) as

$$\Omega_m = 1 - x_1 - x_2 - x_3 - x_4, \quad (45)$$

$$\Omega_G = x_1 + x_2 + x_3, \quad (46)$$

where $\Omega_m = \frac{\rho_m}{3H^2}$ and $\Omega_G = \frac{\rho_G}{3H^2}$. Also we have $\Omega_m + \Omega_r + \Omega_G = 1$.

From Eqs. (15) and (16), one can rewrite ω_G and ω_{eff} in terms of the variables x_i as

$$\omega_G = \frac{-2x_5 - x_4 - 1}{3(x_1 + x_2 + x_3)}, \quad (47)$$

$$\omega_{\text{eff}} = -\frac{1}{3}(2x_5 + 1). \quad (48)$$

Also the deceleration parameter takes the form

$$q = -1 - \frac{\dot{H}}{H^2} = -x_5, \quad (49)$$

and

$$H^6 f_{\text{GG}} = \frac{mx_1}{192 x_5^2}. \quad (50)$$

Notice that in the context of $f(G)$ -gravity, the quantity $H^6 f_{\text{GG}}$ plays an important role. In a viable $f(G)$ model, the condition $0 < H^6 f_{\text{GG}} < 1/384$ is necessary in order to have a stable de Sitter point [15].

From Eqs. (13) and (14), the energy density and pressure due to the $f(G)$ contribution can be expressed in terms of the variables x_i as

$$\rho_G = 3H^2(x_1 + x_2 + x_3), \quad (51)$$

$$p_G = -H^2(2x_5 + x_4 + 1). \quad (52)$$

With the help of Eqs. (32)-(43), the GSL (30) reads

$$T_A \dot{S}_{\text{tot}} = 2\pi\{2x_5[3(x_1 + x_2 - 1) - (x_4 + x_5)] + x_3(5x_5 - 1) + 2\}. \quad (53)$$

Therefore for a given $f(G)$ model, solving the set of first order differential equations (38)-(43) numerically, one can obtain the evolutionary behaviours of H , G , Ω_m , Ω_G , ω_G , ω_{eff} , q and $T_A \dot{S}_{\text{tot}}$. In what follows, we investigate the dynamics of two viable $f(G)$ models and examine the validity of the GSL, i.e. $T_A \dot{S}_{\text{tot}} \geq 0$.

5 Two viable $f(G)$ models

Here, we are interested in investigating the GSL in two viable $f(G)$ models. The first model has the form [14]

$$f(G) = \alpha \left(G^{\frac{3}{4}} - \beta \right)^{\frac{2}{3}}, \quad \text{Model I}, \quad (54)$$

where α and β are two constants of the model. The second $f(G)$ model is given by [15]

$$f(G) = \lambda \frac{G}{\sqrt{G_*}} \arctan \left(\frac{G}{G_*} \right) - \frac{\lambda}{2} \sqrt{G_*} \ln \left(1 + \frac{G^2}{G_*^2} \right) - \alpha \lambda \sqrt{G_*}, \quad \text{Model II}, \quad (55)$$

where α is an arbitrary constant and λ is a positive constant. Also $G_* = H_0^4$ and H_0 is the Hubble parameter at present.

With choice of suitable initial conditions, we numerically solve the differential equations (38)-(43) for both model I and model II. The evolutions of the Hubble parameter H , the Gauss-Bonnet curvature invariant term $|G|$ and the quantity $H^6 f_{\text{GG}}$, Eqs. (36), (37) and (50), versus

$N = \ln(a/a_i)$ for model I and model II are plotted in Figs. 1 and 2, respectively. Figures show that: (i) the Hubble parameter decreases during history of the universe. (ii) The Gauss-Bonnet curvature invariant term changes its sign when it transits from the standard radiation/matter dominated epochs to the accelerated era. (iii) The quantity $H^6 f_{\text{GG}}$ satisfies the condition $0 < H_1^6 f_{\text{GG}}(G_1) < 1/384$ which shows that both models have a stable de Sitter attractor. (iv) H , $|G|$ and $H^6 f_{\text{GG}}$ at late times go to a constant value when the universe enters a de Sitter regime. Notice that the result of Fig. 2 for model II is the same as that obtained in [15].

The evolutions of the density parameters Ω_r , Ω_m , Ω_G and the effective EoS parameter ω_{eff} , Eqs. (45), (46) and (48), versus N for model I and model II are plotted in Figs. 3 and 4, respectively. Figures illustrate that: (i) for both models, Ω_r , Ω_m , Ω_G and ω_{eff} behave like the Λ CDM model in the radiation/matter dominated epochs. (ii) For model I, ω_{eff} oscillates rapidly during the accelerated epoch and goes deep into the phantom-like region as the universe enters the de Sitter period. (iii) For model II, ω_{eff} oscillates slowly around -1 as the system enters the epoch of cosmic acceleration, which implies that the de Sitter solution is a stable spiral. Note that the results of Figs. 3 and 4 are the same as those obtained in [14] and [15], respectively.

The evolutionary behavior of the EoS parameter ω_G due to the $f(G)$ contribution, Eq. (47), for model I and model II is plotted in Figs. 5 and 6, respectively. Figures present that ω_G oscillates quickly at early times and approaches a de Sitter regime at late times, as expected.

The evolution of the deceleration parameter q , Eq. (49), for model I and model II is plotted in Figs. 7 and 8, respectively. Figure 7 clears that for model I, the deceleration parameter starts from $q = 1$ corresponding to the radiation dominated epoch, then shows a cosmic deceleration ($q > 0$) to acceleration ($q < 0$) transition [42] and finally oscillates rapidly into the de Sitter regime ($q = -1$). Figure 8 presents that for model II, q varies from the matter dominated epoch ($q = 0.5$), then transits from a cosmic deceleration to acceleration and approaches smoothly a de Sitter regime at late times, as expected.

In addition, we turn to check the energy conditions in both model I and model II. The energy conditions are as follows [43, 44, 45]:

- (i) The null energy condition (NEC), i.e. $\rho_G + p_G \geq 0$.
- (ii) The strong energy condition (SEC), i.e. $\rho_G + p_G \geq 0$ and $\rho_G + 3p_G \geq 0$.
- (iii) The weak energy condition (WEC), i.e. $\rho_G + p_G \geq 0$ and $\rho_G \geq 0$.
- (iv) The dominant energy condition (DEC), i.e. $\rho_G \geq 0$ and $\rho_G \geq |p_G|$.

Using Eqs. (51) and (52) the evolutionary behaviors of $\rho_G + p_G$, $\rho_G + 3p_G$, ρ_G and $|p_G|$ versus N are plotted in Figs. 9–16. Figures 9, 11, 13 and 15 illustrate that for model I, the energy conditions during the standard radiation/matter dominated epochs are violated in some ranges of N . Thereafter, $\rho_G + p_G$, $\rho_G + 3p_G$, ρ_G and $|p_G|$ oscillate rapidly and finally the energy conditions, but the SEC, for model I are satisfied in the late times. Figures 10, 12, 14 and 16 show that the energy conditions for model II behave like model I. But the difference is that in the future, $\rho_G + p_G$, $\rho_G + 3p_G$, ρ_G and $|p_G|$ for model II vary smoothly when the universe approaches a de Sitter regime.

Finally, we examine the validity of the GSL for both models. In Figs. 17 and 18, we plot the variation of the GSL, Eq. (53), versus N for model I and model II, respectively. Figures illustrate that for both models, the GSL during the radiation/matter dominated epochs is fulfilled. Thereafter when the universe enters the cosmic acceleration era, i.e. $q < 0$ see Figs. 7 and 8, the GSL does not hold (i.e. $T_A \dot{S}_{\text{tot}} < 0$) in some ranges of N . At late times, the GSL for model I oscillates rapidly and for model II approaches smoothly into the de Sitter universe, adiabatically (i.e. $T_A \dot{S}_{\text{tot}} = 0$).

6 Conclusions

Here, we investigated the GSL of gravitational thermodynamics in the framework of $f(G)$ -gravity. To do so, we considered a spatially flat FRW universe filled with the pressureless matter and radiation. We supposed the boundary of the universe to be enclosed by the dynamical apparent horizon with the Hawking radiation. We derived a general relation for the GSL which its validity depends on $f(G)$ -model. Hence, for two viable $f(G)$ -models containing $f(G) = \alpha \left(G^{\frac{3}{4}} - \beta\right)^{\frac{2}{3}}$ [14] and $f(G) = \lambda \frac{G}{\sqrt{G_*}} \arctan\left(\frac{G}{G_*}\right) - \frac{\lambda}{2} \sqrt{G_*} \ln\left(1 + \frac{G^2}{G_*^2}\right) - \alpha \lambda \sqrt{G_*}$ [15], we first solved numerically the set of differential equations governing the dynamics of $f(G)$ -gravity. Consequently, we obtained the evolutionary behaviors of the Hubble parameter, the Gauss-Bonnet curvature invariant term, the pressureless matter, radiation and DE density parameters, the effective EoS parameter and the EoS parameter due to the $f(G)$ contribution as well as the deceleration parameter. In addition, we turned to check the energy conditions containing the NEC, SEC, WEC and DEC. Finally, we examined the validity of the GSL for the two selected $f(G)$ -models. Our results show the following.

(i) The Hubble parameter H , the Gauss-Bonnet curvature invariant term $|G|$ and the quantity $H^6 f_{GG}$ for both models at late times go to a constant value when the universe enters a de Sitter regime. Also both models have a stable de Sitter attractor, because $H^6 f_{GG}$ satisfies the condition $0 < H_1^6 f_{GG}(G_1) < 1/384$.

(ii) The density parameters Ω_r , Ω_m and Ω_G for both models behave quite similar to those of the Λ CDM model in the radiation and matter dominated epochs.

(iii) The EoS parameters ω_{eff} and ω_G for both models start from the radiation/matter dominated epochs, then enter the phantom region (i.e. $\omega < -1$) before reaching the de Sitter attractor with $\omega = -1$.

(iv) The two selected $f(G)$ models can give rise to a late time accelerated expansion phase of the universe. The deceleration parameter for both models shows a cosmic deceleration $q > 0$ to acceleration $q < 0$ transition which is compatible with the observations [42]. Also for both models, q is ended with a stable de Sitter era (i.e. $q \rightarrow -1$).

(v) The NEC, SEC, WEC and DEC for both models during the radiation/matter dominated eras are violated in some ranges of scale factor. But in the late times when the universe approaches a de Sitter regime, the all energy conditions, but the SEC, are satisfied.

(vi) The GSL is fulfilled for both models during the standard radiation/matter dominated epochs. But when the universe becomes accelerating, the GSL is violated (i.e. $T_A \dot{S}_{\text{tot}} < 0$) in some ranges of scale factor. At late times, the evolution of the GSL predicts an adiabatic behavior (i.e. $T_A \dot{S}_{\text{tot}} = 0$) for the accelerated expansion of the universe.

Acknowledgements

The work of A. Abdolmaleki has been supported financially by Center for Excellence in Astronomy & Astrophysics of Iran (CEAAI-RIAAM) under research project No. 1/3927.

References

- [1] M. Kowalski, et al. (Supernova Cosmology Project), *Astrophys. J.* **686**, 749 (2008).

- [2] H. Lampeitl, et al., *Mon. Not. R. Astron. Soc.* **401**, 2331 (2010).
- [3] E. Komatsu, et al. (WMAP Collaboration), *Astrophys. J. Suppl. Ser.* **192**, 18 (2011);
G. Hinshaw, et al. (WMAP Collaboration), *Astrophys. J. Suppl. Ser.* **208**, 19 (2013).
- [4] P.A.R. Ade, et al. (Planck Collaboration), *Astron. Astrophys.* **571**, A16 (2014).
- [5] A.G. Riess, et al., *Astrophys. J.* **699**, 539 (2009).
- [6] T. Padmanabhan, *Phys. Rep.* **380**, 235 (2003);
P.J.E. Peebles, B. Ratra, *Rev. Mod. Phys.* **75**, 559 (2003);
C.G. Tsagas, A. Challinor, R. Maartens, *Phys. Rep.* **465**, 61 (2008);
M. Li, X.D. Li, S. Wang, Y. Wang, *Commun. Theor. Phys.* **56**, 525 (2011).
- [7] V. Sahni, *Class. Quantum Grav.* **19**, 3435 (2002);
E.J. Copeland, M. Sami, S. Tsujikawa, *Int. J. Mod. Phys. D* **15**, 1753 (2006);
T. Padmanabhan, *Gen. Relativ. Gravit.* **40**, 529 (2008).
- [8] S. Capozziello, M.D. Laurentis, *Phys. Rep.* **509**, 167 (2011);
T. Clifton, P.G. Ferreira, A. Padilla, C. Skordis, *Phys. Rep.* **513**, 1 (2012).
- [9] S. Nojiri, S.D. Odintsov, *Phys. Rev. D* **68**, 123512 (2003);
T.P. Sotiriou, V. Faraoni, *Rev. Mod. Phys.* **82**, 451 (2010);
S. Nojiri, S.D. Odintsov, *Phys. Rep.* **505**, 59 (2011);
K. Karami, M.S. Khaledian, *JHEP* **03**, 086 (2011).
- [10] S. Nojiri, S.D. Odintsov, *Phys. Lett. B* **631**, 1 (2005).
- [11] G.R. Bengochea, R. Ferraro, *Phys. Rev. D* **79**, 124019 (2009);
K. Karami, A. Abdolmaleki, S. Asadzadeh, Z. Safari, *Eur. Phys. J. C* **73**, 2565 (2013);
K. Karami, S. Asadzadeh, A. Abdolmaleki, Z. Safari, *Phys. Rev. D* **88**, 084034 (2013);
K. Karami, A. Abdolmaleki, *Res. Astron. Astrophys.* **13**, 757 (2013).
- [12] Y. Sobouti, *Astron. Astrophys.* **464**, 921 (2007).
- [13] B. Li, J.D. Barrow, D.F. Mota, *Phys. Rev. D* **76**, 044027 (2007);
S.C. Davis, *Prog. Theor. Phys. Suppl.* **172**, 81 (2008).
- [14] S.Y. Zhou, E.J. Copeland, P.M. Saffin, *JCAP* **07**, 009 (2009).
- [15] A. De Felice, S. Tsujikawa, *Phys. Lett. B* **675**, 1 (2009).
- [16] A. De Felice, S. Tsujikawa, *Living Rev. Relativity* **13**, 3 (2010).
- [17] A. De Felice, M. Hindmarsh, M. Trodden, *JCAP* **08**, 005 (2006).
- [18] G. Cognola, E. Elizalde, S. Nojiri, S. Odintsov, S. Zerbini, *Phys. Rev. D* **75**, 086002 (2007);
S. Nojiri, S.D. Odintsov, P.V. Tretyakov, *Prog. Theor. Phys. Suppl.* **172**, 81 (2008).
- [19] R.M. Wald, *Phys. Rev. D* **48**, 3427 (1993);
S.M. Carroll, et al., *Phys. Rev. D* **71**, 063513 (2005);
G. Cognola, E. Elizalde, S. Nojiri, S.D. Odintsov, S. Zerbini, *JCAP* **02**, 010 (2005).
- [20] M. Alimohammadi, A. Ghalee, *Phys. Rev. D* **79**, 063006 (2009);
M. Alimohammadi, A. Ghalee, *Phys. Rev. D* **80**, 043006 (2009).

- [21] R.R. Metsaev, A.A. Tseytlin, Nucl. Phys. B **293**, 385 (1987).
- [22] J.D. Bekenstein, Phys. Rev. D **7**, 2333 (1973);
S.W. Hawking, Commun. Math. Phys. **43**, 199 (1975).
- [23] T. Jacobson, Phys. Rev. Lett. **75**, 1260 (1995).
- [24] R.G. Cai, S.P. Kim, JHEP **02**, 050 (2005).
- [25] M. Akbar, R.G. Cai, Phys. Lett. B **635**, 7 (2006);
M. Akbar, R.G. Cai, Phys. Lett. B **648**, 243 (2007).
- [26] R.X. Miao, M. Li, Y.G. Miao, JCAP **11**, 033 (2011).
- [27] M. Akbar, R.G. Cai, Phys. Rev. D **75**, 084003 (2007).
- [28] A. Sheykhi, JCAP **05**, 019 (2009).
- [29] G. Izquierdo, D. Pavón, Phys. Lett. B **639**, 1 (2006).
- [30] H. Mohseni Sadjadi, Phys. Rev. D **73**, 063525 (2006);
H. Mohseni Sadjadi, Phys. Rev. D **76**, 104024 (2007);
H. Mohseni Sadjadi, Phys. Lett. B **645**, 108 (2007).
- [31] J. Zhou, B. Wang, Y. Gong, E. Abdalla, Phys. Lett. B **652**, 86 (2007).
- [32] Y. Gong, B. Wang, A. Wang, Phys. Rev. D **75**, 123516 (2007);
Y. Gong, B. Wang, A. Wang, JCAP **01**, 024 (2007).
- [33] A. Sheykhi, B. Wang, Phys. Lett. B **678**, 434 (2009);
A. Sheykhi, B. Wang, Mod. Phys. Lett. A **25**, 1199 (2010);
A. Sheykhi, Phys. Rev. D **81**, 104011 (2010);
A. Sheykhi, Eur. Phys. J. C **69**, 265 (2010);
A. Sheykhi, Class. Quantum Grav. **27**, 025007 (2010).
- [34] K. Karami, JCAP **01**, 015 (2010);
K. Karami, S. Ghaffari, M.M. Soltanzadeh, Class. Quantum Grav. **27**, 205021 (2010);
K. Karami, A. Sheykhi, N. Sahraei, S. Ghaffari, Europhys. Lett. **93**, 29002 (2011);
K. Karami, A. Abdolmaleki, N. Sahraei, S. Ghaffari, JHEP **08**, 150 (2011).
- [35] N. Radicella, D. Pavón, Phys. Lett. B **691**, 121 (2010).
- [36] K. Karami, A. Abdolmaleki, JCAP **04**, 007 (2012);
A. Abdolmaleki, T. Najafi, K. Karami, Phys. Rev. D **89**, 104041 (2014).
- [37] K. Bamba, C.Q. Geng, JCAP **11**, 008 (2011).
- [38] S. Capozziello, V.F. Cardone, S. Carloni, A. Troisi, Int. J. Mod. Phys. D **12**, 1969 (2003);
S. Capozziello, V.F. Cardone, A. Troisi, Phys. Rev. D **71**, 043503 (2005).
- [39] E. Poisson, W. Israel, Phys. Rev. D **41**, 1796 (1990);
S.A. Hayward, Phys. Rev. D **53**, 1938 (1996);
Y.G. Gong, A. Wang, Phys. Rev. Lett. **99**, 211301 (2007).
- [40] R.G. Cai, L.M. Cao, Y.P. Hu, Class. Quantum Grav. **26**, 155018 (2009).

- [41] J.J. Halliwell, Phys. Lett. B **185**, 341 (1987);
E.J. Copeland, A.R. Liddle, D. Wands, Phys. Rev. D **57**, 4686 (1998);
S.Y. Zhou, Phys. Lett. B **660**, 7 (2008).
- [42] E.E. Ishida, R.R.R. Reis, A.V. Toribio, I. Waga, Astropart. Phys. **28**, 547 (2008).
- [43] S.W. Hawking, G.F.R. Ellis, *The Large Scale Structure of Spacetime*, Cambridge University Press (1973);
R.M. Wald, *General Relativity*, The University of Chicago Press (1984).
- [44] K. Bamba, S. Nojiri, S.D. Odintsov, JCAP **10**, 045 (2008);
N.M. Garcia, T. Harko, F.S.N. Lobo, J.P. Mimoso, Phys. Rev. D **83**, 104032 (2011).
- [45] J.D. Barrow, Class. Quantum Grav. **21**, L79 (2004);
S. Nojiri, S.D. Odintsov, S. Tsujikawa, Phys. Rev. D **71**, 063004 (2005).

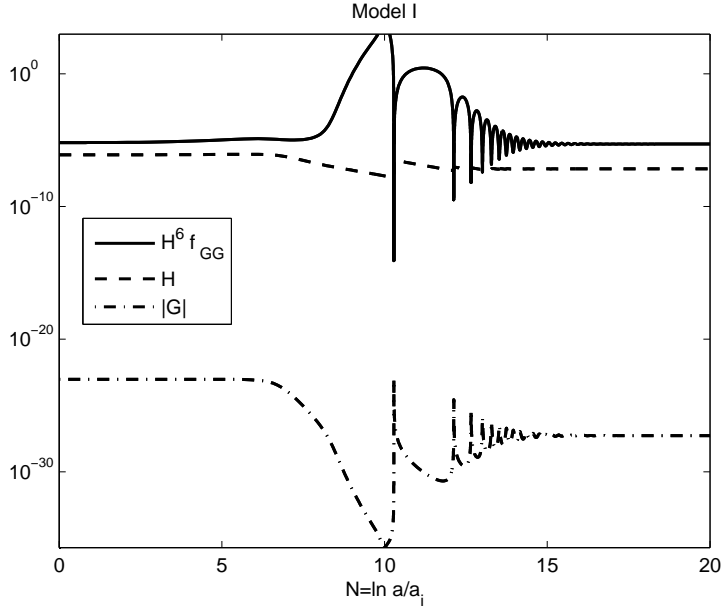


Figure 1: The evolutions of the Hubble parameter H , the Gauss-Bonnet curvature invariant term $|G|$ and the quantity $H^6 f_{GG}$, Eqs. (36), (37) and (50), versus $N = \ln(a/a_i)$ where a_i is the initial value of the scale factor. Auxiliary parameters are: $\alpha = \frac{1}{40\sqrt{66}}$ and $\beta = -10^{-17}$. Initial values are: $x_1 = -0.0025$, $x_2 = 0.005$, $x_3 = -0.01$, $x_4 = 0.99951$, $x_5 = -0.99$ [14] and $x_6 = 7.95225 \times 10^{-7}$.

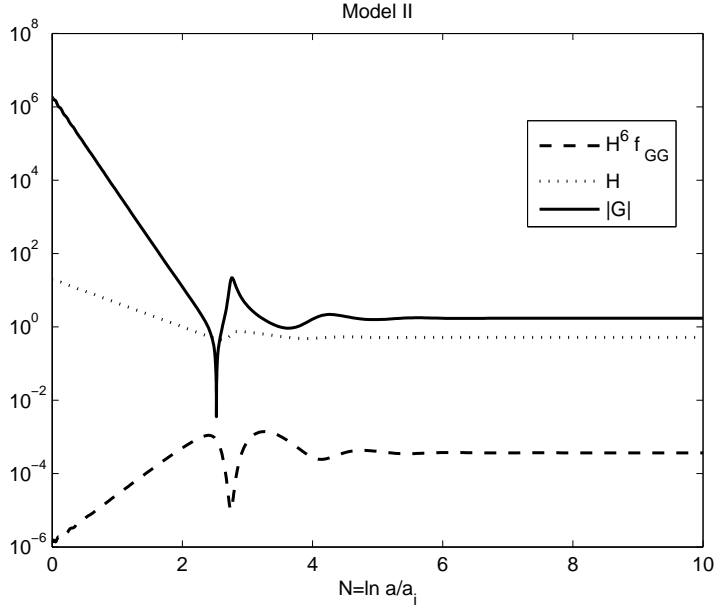


Figure 2: Same as Fig. 1 but for model II. Auxiliary parameters are: $\alpha = 10$ and $\lambda = 0.075$ [15]. Initial values are: $x_1 = 189.249$, $x_2 = -189.248$, $x_3 = -0.0014$, $x_4 = 0.004$, $x_5 = -0.502$ and $x_6 = 20$.

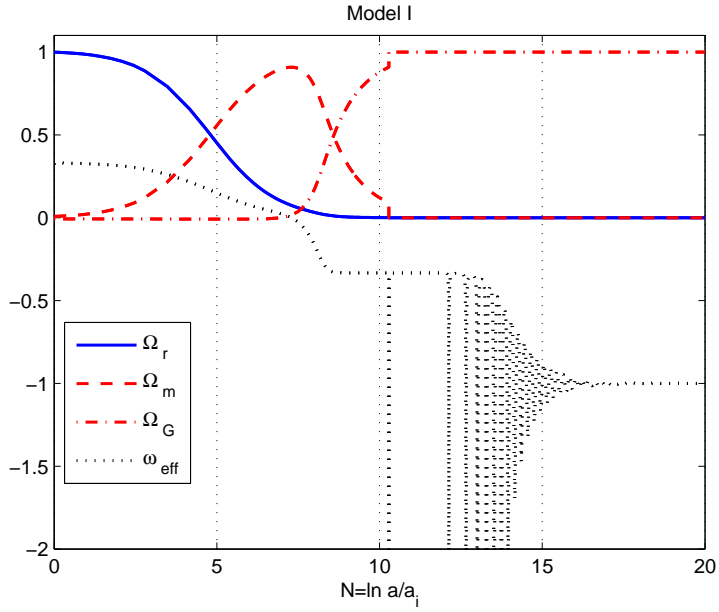


Figure 3: The evolutions of Ω_m , Ω_G , Ω_r and ω_{eff} , Eqs. (45), (46) and (48), versus N . Auxiliary parameters and initial values as in Fig. 1.

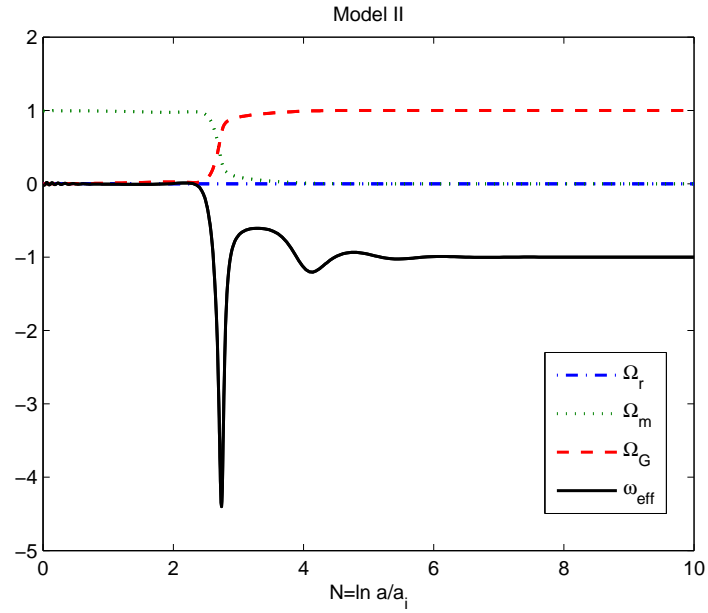


Figure 4: Same as Fig. 3 but for model II. Auxiliary parameters and initial values as in Fig. 2.

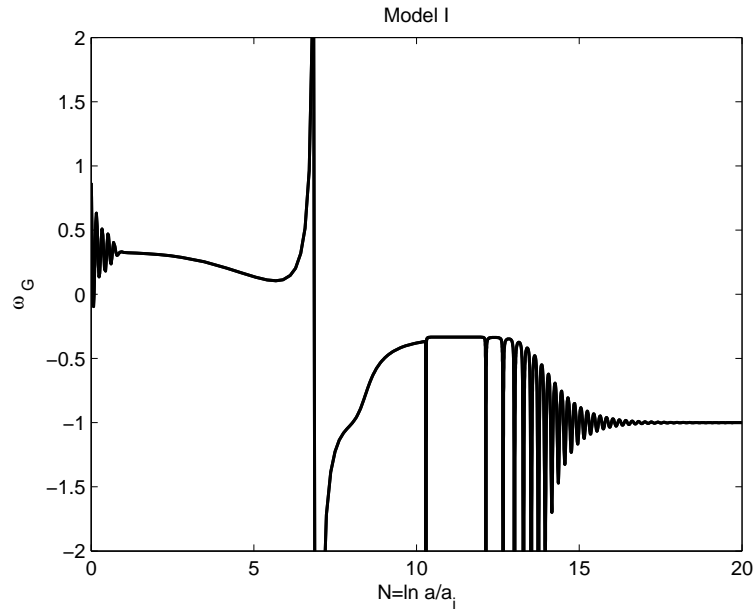


Figure 5: The evolution of the EoS parameter ω_G , Eq. (47), versus N for model I. Auxiliary parameters and initial values as in Fig. 1.

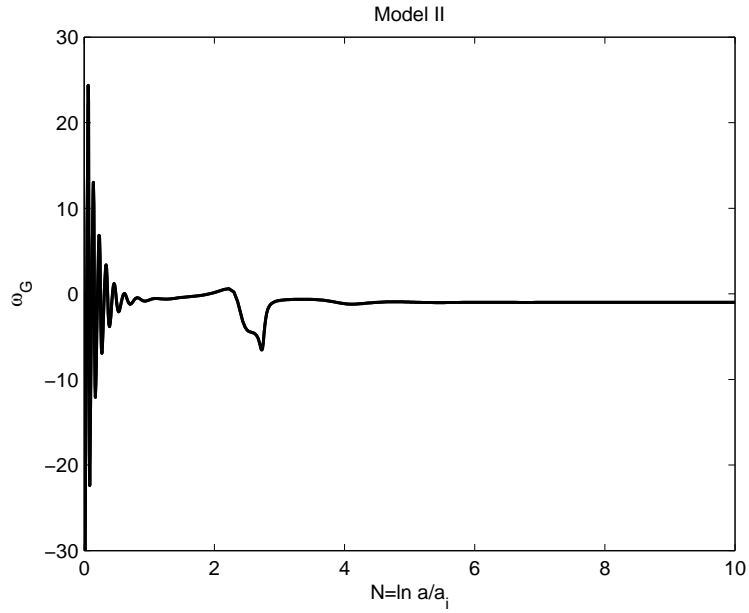


Figure 6: Same as Fig. 5 but for model II. Auxiliary parameters and initial values as in Fig. 2.

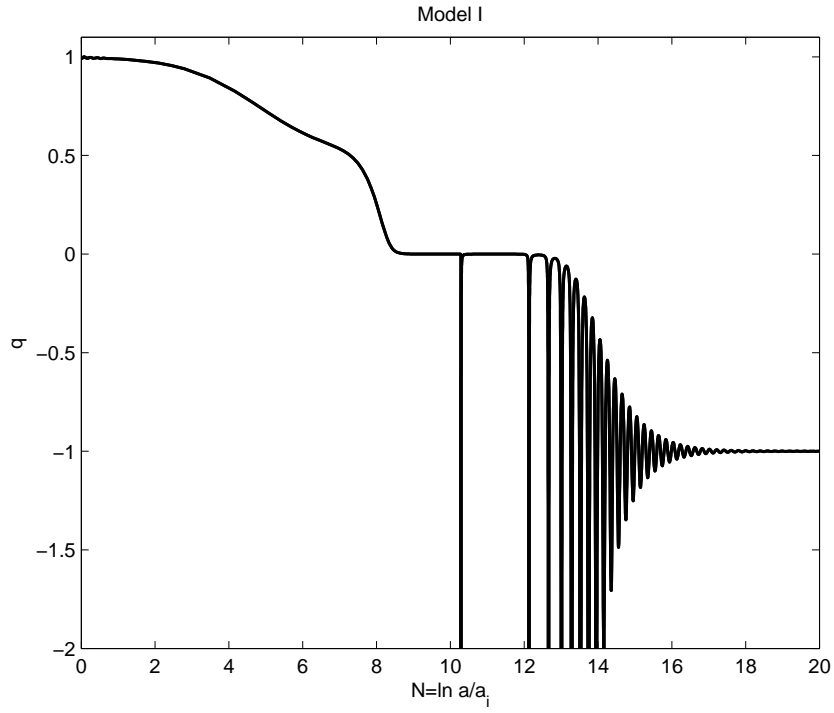


Figure 7: The evolution of the deceleration parameter q , Eq. (49), versus N for model I. Auxiliary parameters and initial values as in Fig. 1.

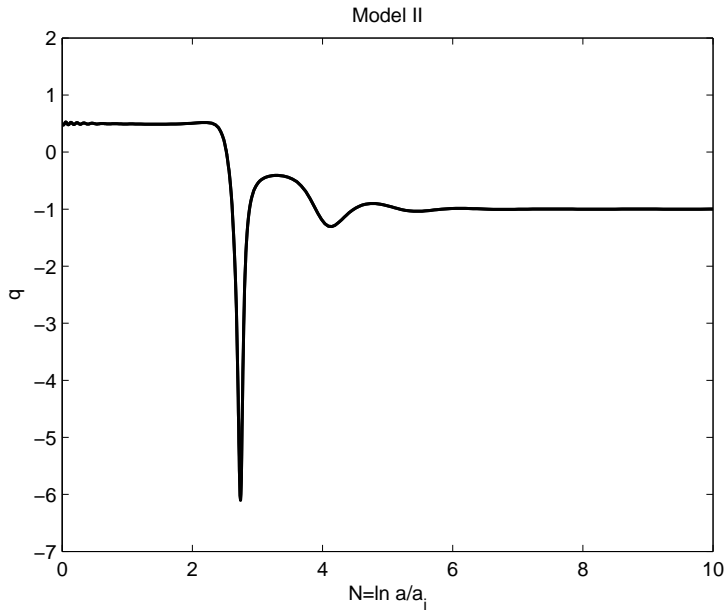


Figure 8: Same as Fig. 7 but for model II. Auxiliary parameters and initial values as in Fig. 2.

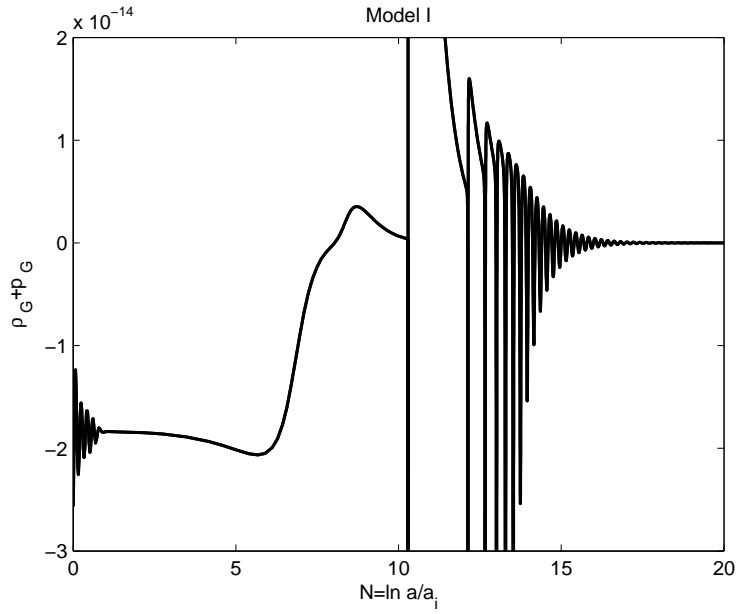


Figure 9: The evolution of $\rho_G + p_G$, Eqs. (51) and (52), versus N for model I. Auxiliary parameters and initial values as in Fig. 1.

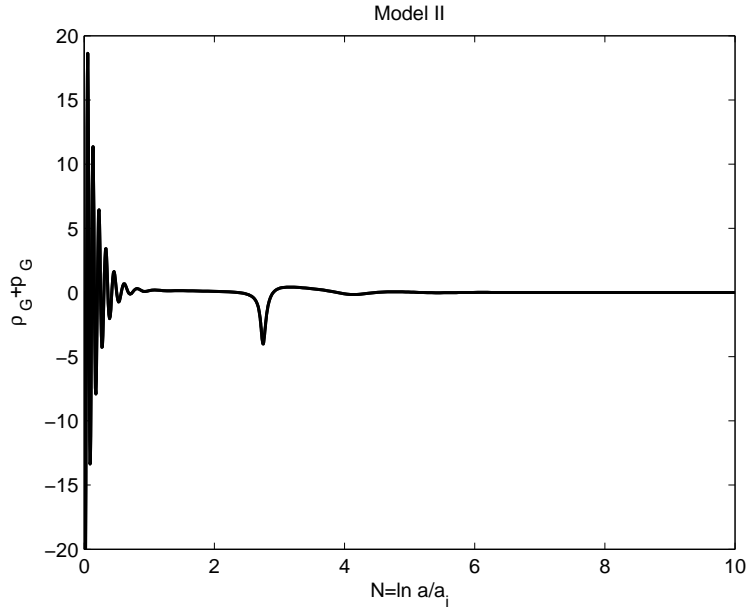


Figure 10: Same as Fig. 9 but for model II. Auxiliary parameters and initial values as in Fig. 2.

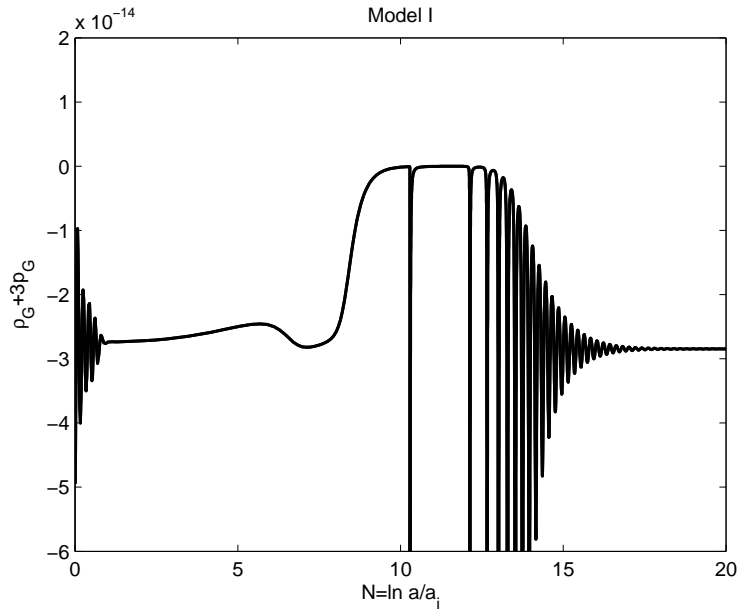


Figure 11: The evolution of $\rho_G + 3p_G$, Eqs. (51) and (52), versus N for model I. Auxiliary parameters and initial values as in Fig. 1.

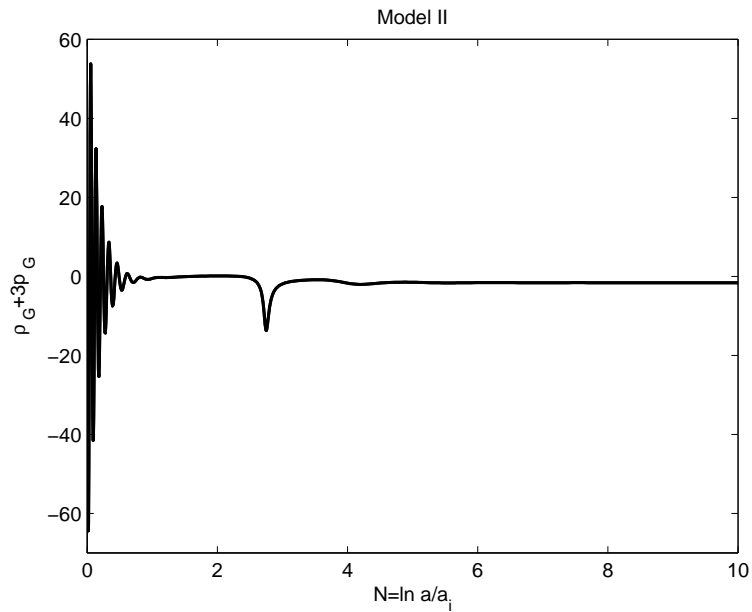


Figure 12: Same as Fig. 11 but for model II. Auxiliary parameters and initial values as in Fig. 2.

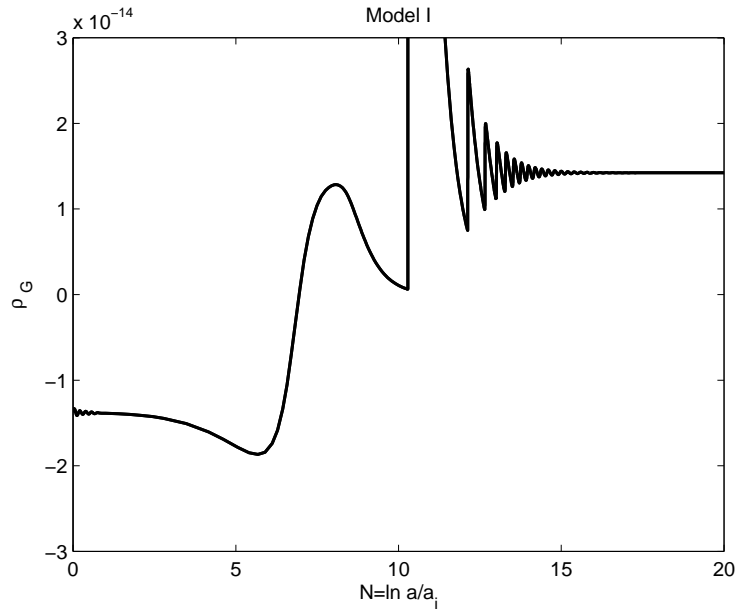


Figure 13: The evolution of ρ_G , Eq. (51), versus N for model I. Auxiliary parameters and initial values as in Fig. 1.

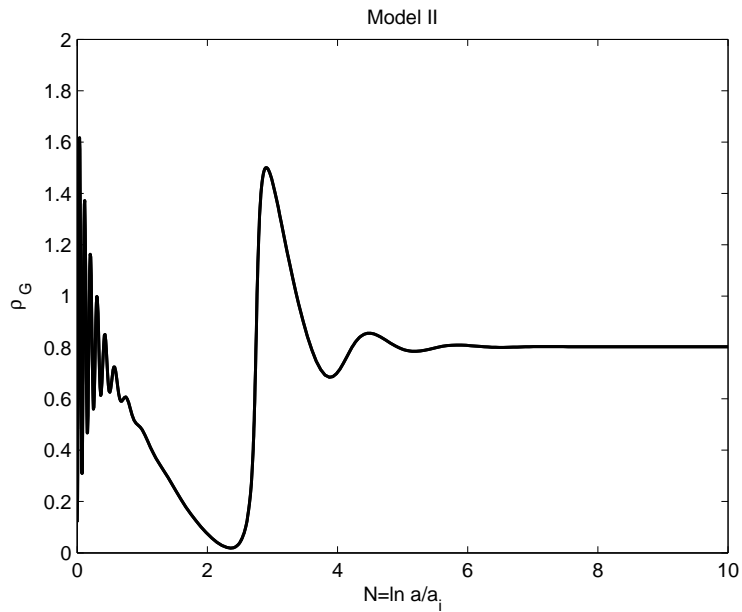


Figure 14: Same as Fig. 13 but for model II. Auxiliary parameters and initial values as in Fig. 2.

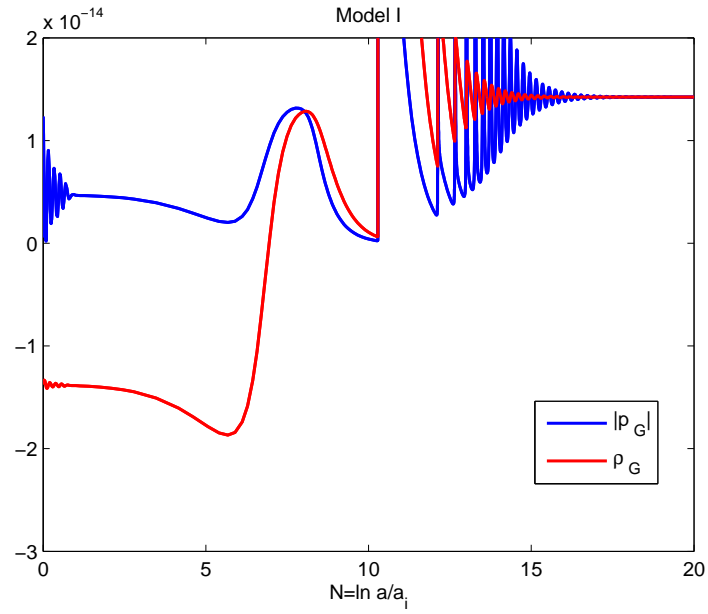


Figure 15: The evolutions of ρ_G and $|p_G|$, Eqs. (51) and (52), versus N for model I. Auxiliary parameters and initial values as in Fig. 1.

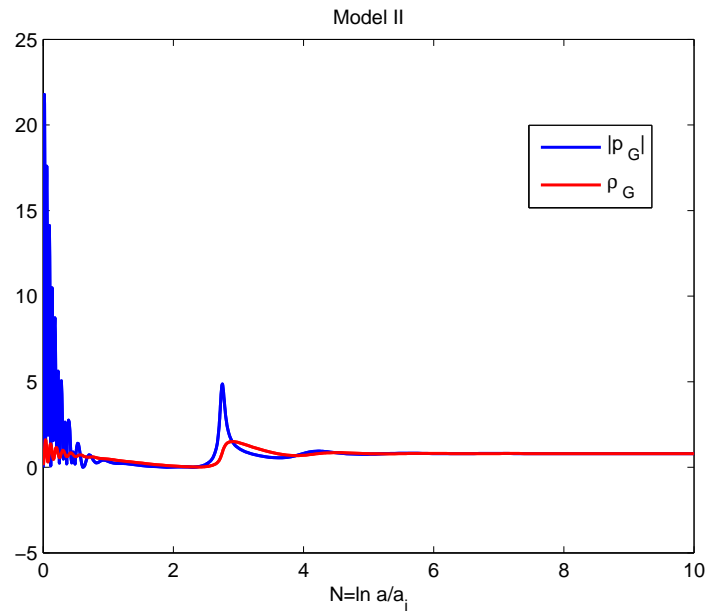


Figure 16: Same as Fig. 15 but for model II. Auxiliary parameters and initial values as in Fig. 2.

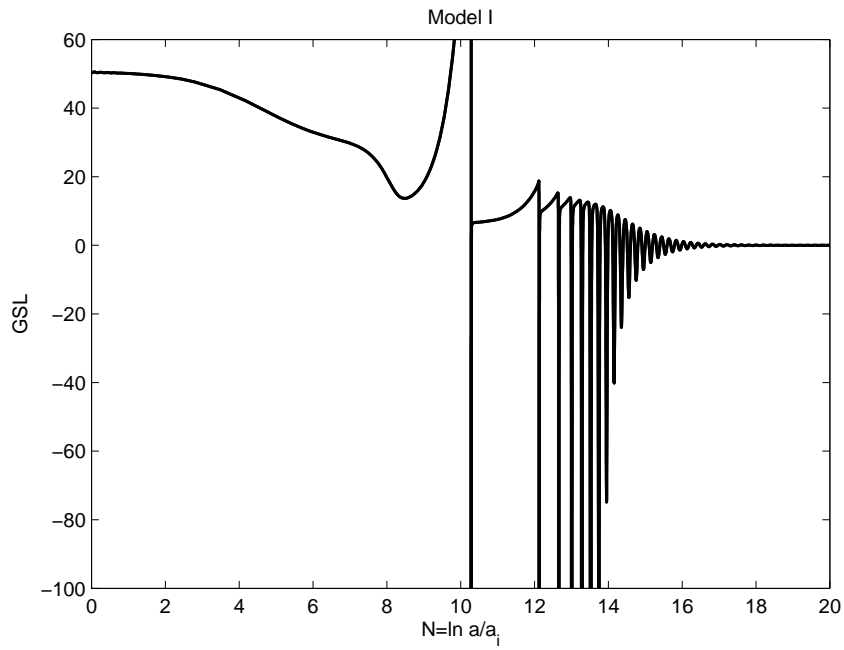


Figure 17: The evolution of the GSL, Eq. (53), versus N for model I. Auxiliary parameters and initial values as in Fig. 1.

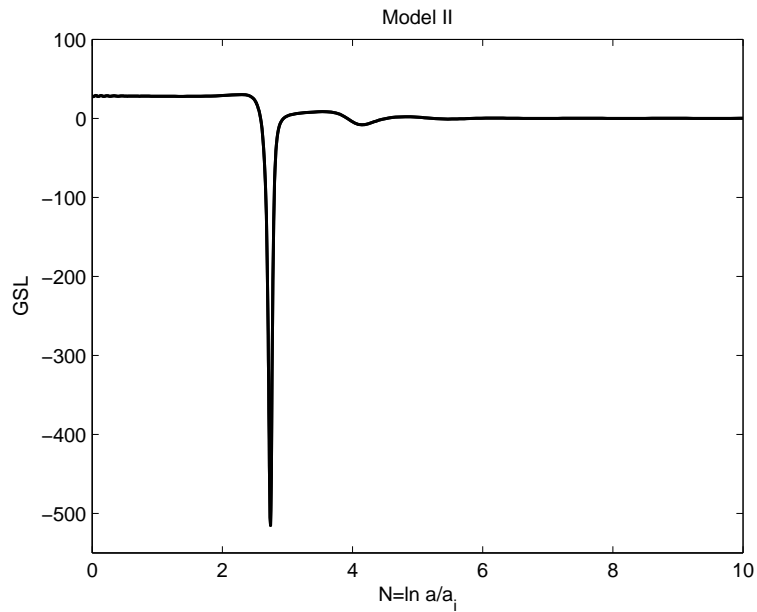


Figure 18: Same as Fig. 17 but for model II. Auxiliary parameters and initial values as in Fig. 2.